

THREE-STEP PROCEDURE TO MEASURE SURFACE ACCURACY OF A PARABOLIC DISH ANTENNA

Joe Martin¹

Espanola, NM 87532

1 March 2022, Rev. 1

ABSTRACT

A three-step procedure to measure the surface accuracy of a parabolic dish antenna is described. A description is given of the use of the procedure to detect defects in the reflecting surface of a 4.63 meter diameter parabolic dish. The information is then used to guide adjustments of the surface curvature of the dish to improve performance at 8.4 GHz. A reduction in angular width of the principal lobe of the dish antenna pattern by a factor of about two and a more than doubling of dish gain is demonstrated. Details of a robotic-turret-mounted laser range finder instrument used to perform the surface measurements and a description of how the surface curvature of the dish was adjusted to achieve improved performance are presented.

I. INTRODUCTION

Imperfections and structural deformations of the reflecting surface of parabolic dish antennas can be a significant source of signal loss and low performance of radio telescopes. Such defects are not easily identified and corrected by users in many cases. Various techniques have been employed by professional radio astronomers to quantitatively characterize the surfaces of parabolic antennas to reveal regions of a reflecting surface that may need mechanical adjustment to achieve optimum antenna performance. Among these techniques are microwave holography², optical photogrammetry³, and laser range finding⁴.

For amateur radio astronomers these techniques are sometimes impractical to implement due to the complexity of the techniques, expense involved in obtaining the equipment, difficulty in performing the measurements and/or difficulty in analyzing the resulting data. However, due to recent availability of relatively inexpensive robotic hardware, laser range-finding modules, versatile serial communication interface modules, and free/open-source software tools to aid in performing data analyses, it is now possible for amateur radio astronomers on restricted budgets to make suitable dish-surface measurements straightforwardly by assembling and using powerful surface-measuring instruments to detect surface defects.

This document describes a three-step procedure using a robotic-turret-mounted laser-rangefinder instrument to measure surface accuracy of a parabolic dish. The steps are:

- 1) Measure distances from the focal point to points on the surface of the dish.**
- 2) Determine a paraboloid reference surface for the dish.**
- 3) Calculate deviations of the dish surface from the reference surface.**

A detailed description of how each of these three steps may be implemented is discussed in this document. The document is organized as follows:

Section I provides a general introduction, Section II describes how each of the three steps may be implemented. Section III describes the curvature modification process used on the example dish. Section IV presents performance measurement results at 8.4 GHz, Section V presents a summary and Section VI lists references. The document concludes with an Appendix that gives our derivation of a formula that is used in Section II.

II. DESCRIPTION OF THE PROCEDURE STEPS

Step 1: Measure distances from the focal point to points on the surface of the dish

The first step consists of measuring the distances from the focal point of the dish to the reflecting surface at numerous points on the dish. As an example to demonstrate the procedure we use a 4.63 meter diameter primary-focus parabolic dish presently being used for radio astronomy at 8.4 GHz. The dish is shown in Figure 1.



Fig. 1 The 4.63 meter diameter dish used as the example for this paper.

A laser rangefinder-based instrument assembled by the author is used to make distance measurements from the focal point of the dish to the dish surface. Figure 2 shows a composite 3-dimensional image of the more than 5,000 points measured using the instrument.

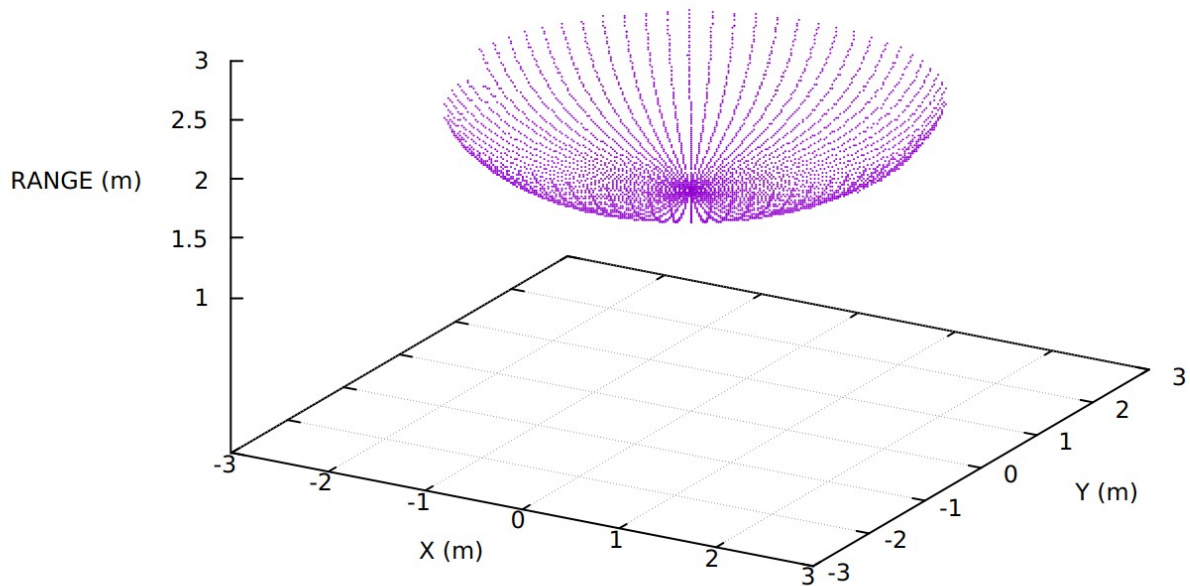


Fig.2 A composite 3-D image of the points measured with the laser rangefinder instrument.

The laser rangefinder-based instrument used to make the measurements is shown in Figure 3, mounted onto an 8" diameter PVC pipe to conveniently and temporarily replace the existing feed horn assembly on the dish. The instrument was mounted at the focal point of the dish to perform the measurements.

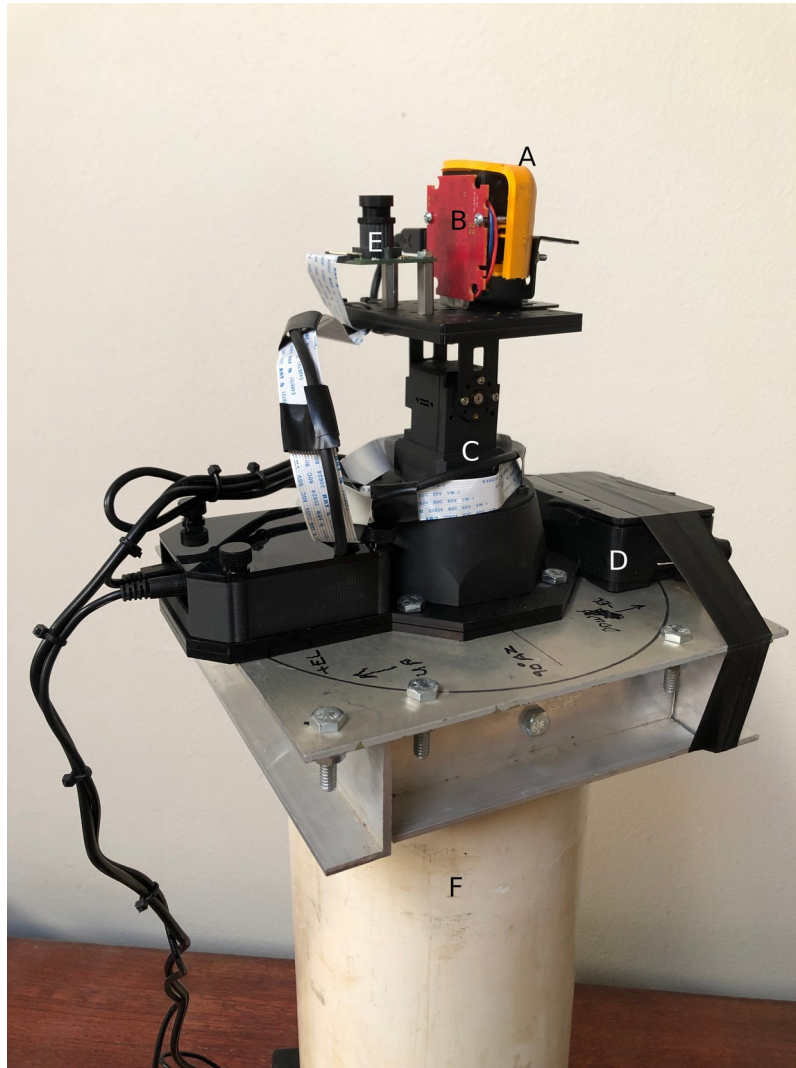


Fig. 3. The robotic-turret-mounted laser rangefinder instrument used for the distance measurements.

Components of the range finding instrument are labeled in the image above and consist of:

- A: The laser board portion of a Fluke 414D Laser Distance Meter⁵
- B: Porcupine Labs LR4-USB interface board⁶
- C: Remote controlled 2-axis robotic pan/tilt “PhantomX” turret assembly⁷
- D: Raspberry Pi 4b computer
- E: Raspberry Pi compatible camera
- F: 8” diameter PVC tube mount

Inter-connections of the instrument components are shown in Figure 4.

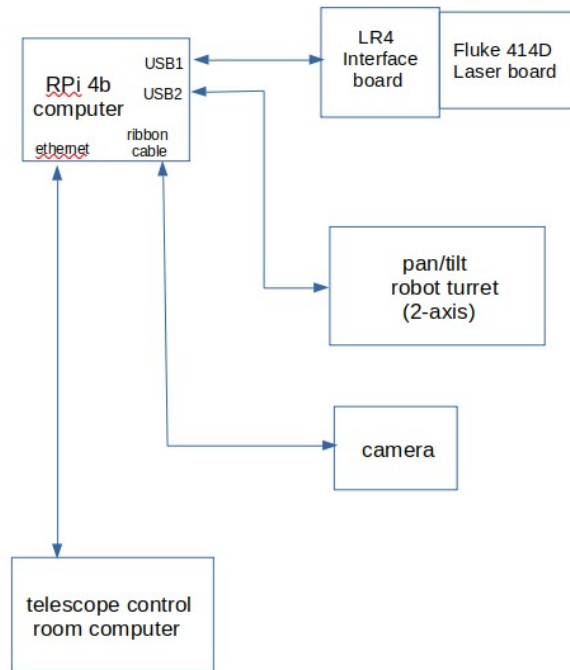


Fig. 4. Diagram showing how the components of the instrument are connected.

The instrument is controlled by a computer program, written in C++ by the author, running on the Raspberry Pi computer (RPi4). The RPi4 is mounted onto the same plate as the robotic pan/tilt turret. Remote interaction with the Raspberry Pi is achieved via ethernet connection from a computer in the telescope control room. The Raspberry Pi desktop display and program control are accessed remotely via a Virtual Network Computing (VNC) connection into the Raspberry Pi computer from the control room computer. While a VNC connection can be established via the wireless WiFi capability of the Raspberry Pi, it was found that a wire ethernet connection between the computers was more reliable and permitted faster responses from the instrument.

The RPi4-compatible camera is used occasionally to verify remotely from the telescope control room that the turret actually moves the laser spot to the proper position when the turret is commanded to move. A camera interface capability is standard in the Raspberry Pi operating system and is used to display images directly on the desktop display as desired, viewed remotely from the telescope control room via the VNC connection to the RPi4. The RPi4 is used in a “headless” configuration; i.e., no display monitor or keyboard is attached to the RPi4.

The instrument is used to measure and record distances from focal point to dish reflecting surface while stepping the tilt axis of the turret in arbitrarily selected 1 degree steps from a near-rim point on the dish surface through the vertex position of the surface to the opposite-side near-rim point at a given pan angle of the turret. Greater or lesser spatial resolution can be obtained by varying the angular step size in the computer program; steps as small as 0.087 degree are possible with the turret used. The time required to measure distance to a point is about 1 second with an accuracy of

about 2mm. We opted to measure each point five times taking the fifth measurement as our data value to allow time for mechanical settling of the turret after a move and to allow stabilizing of the rangefinder for each measurement position. The collection of measurements, representing a single “scan” across the dish surface, is saved as a data file consisting of a list of 3-dimensional points that is readable by most spreadsheet programs. Each line entry in a data file consists of three elements a,b,c specifying a point in three dimensions; these are

- a = pan angle of the turret,
- b = tilt angle of the turret, and
- c = distance to the dish surface.

After completing a scan the pan angle of the turret is incremented by whatever increment is needed to achieve the desired angular separation between measured scans, in our case we chose 5 degrees, and a new tilt-angle scan is initiated producing another scan across the surface and a another data file of 3-D measurements. The pan angle is incremented through a 180-degree range from -90 degrees to +90 degrees, in 5 degree steps in our case, to sample points over the entire dish surface in 36 tilt-angle “scans”. We arbitrarily defined the 360-degree rotation of the turret pan angle into a range of -180 to +180 degrees; however, as the top platform of the turret is able to move in tilt angle through a range greater than -90 to +90 degrees, i.e., it can move to either side of the top center position, a range of only -90 to +90 degrees for pan angle covers the entire dish surface (and more in this particular case) by the laser when using rim-to-rim scans in tilt angle.

For this dish, each rim-to-rim scan uses tilt angles ranging from -73 degrees to +73 degrees in 1-degree steps, or in whatever increment is selected to achieve the desired spatial resolution between measured points. A 73 degree tilt angle puts the laser position near a rim-edge position on the dish. Time required to complete measurements over the entire surface of this dish at the angular spacing between points we selected is about six hours. If lesser resolution is acceptable the time needed to acquire measurements of the dish surface is reduced accordingly.

Figure 5 shows a view along the z-axis of the dish so that the reader can obtain a perspective and sense of orientation of the physical elements present on the dish with respect to the measured points.



Fig. 5. Image showing orientation of the x and y axes used during the data analyses.

The selected spacing of the measured points obtained during the scans across the dish, oriented as shown in Figure 5, provide a large number of points from which to determine the local curvature over the entire surface of the dish. A projection of the measured points onto the x-y plane are shown in Figure 6.

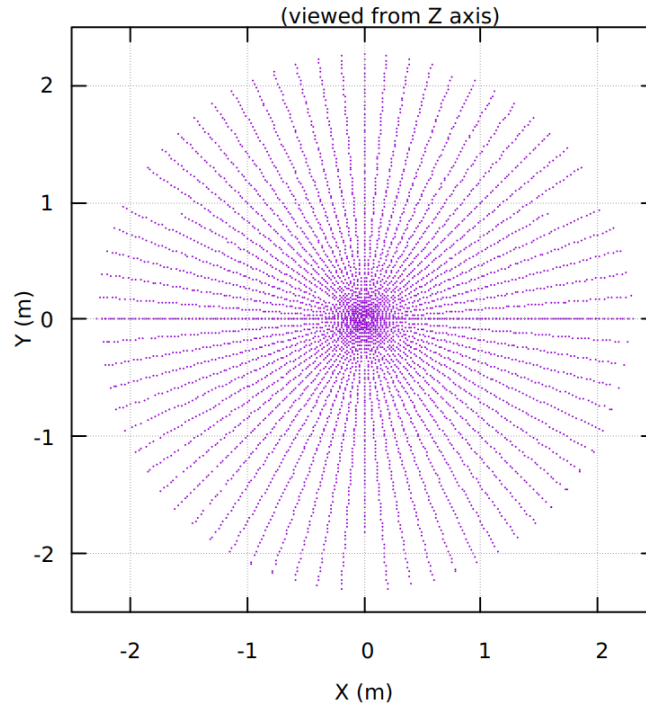


Fig. 6. An x-y plane projection of the measured points on the dish. Note that a portion of the scans during which the laser was blocked by the feed horn support beams are shortened with respect to scans that were not blocked. The partially blocked scans appear at 120 degree intervals in the image.

The measured points are used in the subsequent analyses in two ways. First, the points will be used to determine a 3-dimensional paraboloid reference surface that describes the average curvature of the dish. Second, the points will be used to determine local deviations from the reference surface so that a plan can be made for correcting the areas of deviation to better match the reference surface. A better match is expected to yield improved dish performance.

Step 2. Determine a paraboloid reference surface

Each of the rim-to-rim scans across the dish surface produce data points that describe a parabola that may be perturbed by local defects in the dish surface. Further, it is important to recognize that the coordinates of the data points, as collected and saved by the instrument, are recorded using an unusual coordinate system. In particular, each point is recorded in terms of “pan angle”, “tilt angle”, and “range”. It is therefore useful to translate those coordinates into a more standard coordinate system, such as the x, y, z orthogonal coordinate system, so that standard analytical techniques may be straightforwardly applied to the data. Figure 7 shows graphically the relationship between elements of the two coordinate systems.

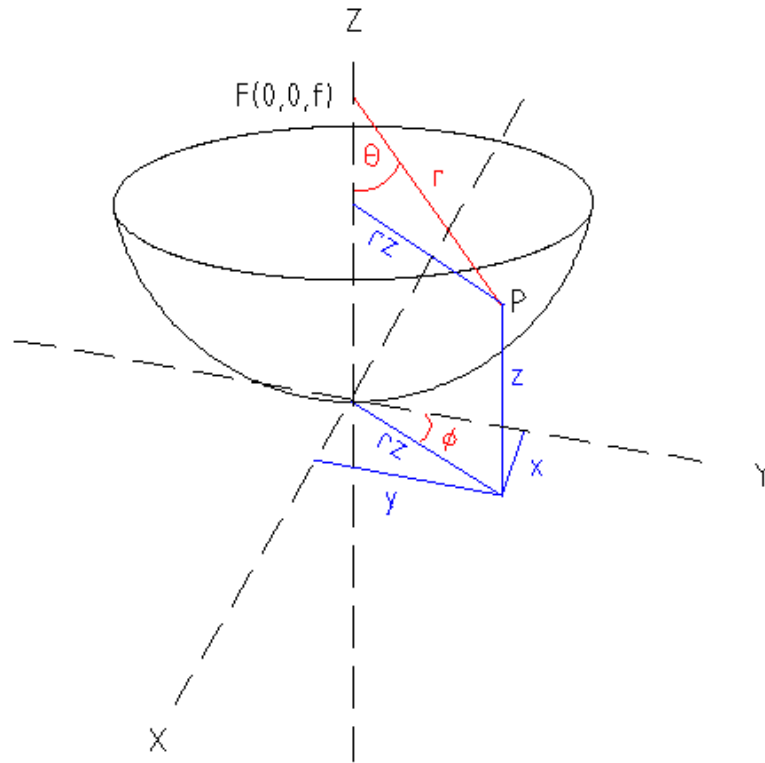


Fig. 7. Diagram showing relationships between the ϕ , θ , r coordinate elements shown in red and the x , y , z coordinate elements shown in blue for a point P on the surface of the dish. Point F is the focal point of the dish at $F(0, 0, f)$.

Point P on the surface of the dish may be represented by either $P(\phi, \theta, r)$ or $P(x,y,z)$, where the coordinates ϕ , θ , r are defined as:

- ϕ = pan angle of the robotic turret
- θ = tilt angle of the robotic turret
- r = range to the surface as measured by the laser rangefinder

Referring to Figure 7, the relationships between elements of the two coordinate systems are therefore:

$$x = rz \sin(\phi) \tag{1}$$

$$y = rz \cos(\phi) \tag{2}$$

$$z = r (1 - \cos(\theta)) / 2 \tag{3}$$

where $rz = r \sin(\theta)$. (4)

“rz” is the the shortest distance from point P to the Z axis. Our derivation of Eqn. 3 is given in the Appendix of this document.

By using Eqns 1-3 one may translate the coordinates of the points that have been measured in the ϕ,θ,r coordinate system to coordinates of the more useful x,y,z coordinate system. Doing so makes possible direct comparisons of the z-components of the measured points with the z-components of corresponding points on a reference surface. “Corresponding”, in this case refers to points on the reference surface that have the same x and y coordinate values as the measured points. Deviations of the z-components of the measured points from the z-components of the reference surface reveal where, in terms of x,y coordinates, the defects lie on the dish surface, and by how much and in which direction, relative to the z-axis, the dish surface deviates from the reference surface. This information is used to guide how mechanical adjustments are applied to the dish in attempts to change the reflecting surface curvature to improve dish performance.

A suitable paraboloid reference surface may now be determined from the measured, coordinate-translated points to permit comparison of the dish surface at all the measured points with corresponding points of a reference surface. However, calculating the coefficients, k_i , for a general-case 3-D paraboloid reference surface of the form

$$k_1x^2 + k_2y^2 + k_3z^2 + k_4xy + k_5yz + k_6zx + k_7x + k_8y + k_9z + k_{10} = 0$$

directly from the huge number of measured points is a complex undertaking typically involving tedious matrix calculations and manipulations, and in the general case of an arbitrarily oriented general-form paraboloid it is not even possible to calculate the ten parameters that are needed to describe the paraboloid using the direct matrix calculation approach⁸. If one constrains the reference paraboloid by insisting it be a centered paraboloid, a matrix solution can be obtained by performing the complex matrix calculations⁹. Fortunately, such general case and near-general-case matrix solutions are not required for us to solve our problem of obtaining a suitable reference surface if we further constrain the reference surface. Indeed, we can completely avoid the complexity of the general case solution by heavily constraining our reference paraboloid appropriately.

The task is dramatically simplified by requiring that the principal axis of our paraboloid be aligned with the z-axis of the dish and that the paraboloid be symmetric about the z-axis of the dish. These two constraints reduce the number of parameters that we must solve for to two, instead of the ten required for the general-case paraboloid.

The constrained reference paraboloid will have the form:

$$z = A(x^2 + y^2) + B, \quad (5)$$

where coefficient A determines the opening angle of the paraboloid and coefficient B determines the position of the vertex of the paraboloid along the z-axis.

The process may be simplified further by calculating a series of best-fit 2-D parabolas from our measured scans, one parabola for each of the scans, instead of trying to determine a 3-D paraboloid directly from all of the data points simultaneously. To do this, note that each of the scans produces a parabola in the plane defined by the z-axis and any point in the scan that does not lie on the z-axis. Each parabola is of the form:

$$z = a_i x^2 + b_i \quad (6)$$

for the i -th scan of our data set. Of course, the parabola produced by each scan will have perturbations from a perfect parabola that reflect local defects in the dish surface, therefore it is desirable to fit each scan to a “best-fit” parabola of the form given by Eqn. 6.

The coefficients a_i and b_i for the i -th scan across the dish are easily determined using standard least-squares techniques to fit the data points in the scan to obtain the two coefficients. Or equivalently, as we opted to do instead, use the linear regression capability of the “R” language computer tool¹⁰ to quickly determine the two coefficients for each scan.

After performing linear regression on all 36 scans to obtain the sets of a_i and b_i values, we calculate the average of the a_i values and the average of the b_i values to obtain the coefficients, A and B , of Eqn. 5 for our reference parabola for the dish. That is,

$$A = \frac{\sum_{i=1}^{36} a_i}{36} , \quad (7)$$

and

$$B = \frac{\sum_{i=1}^{36} b_i}{36} ; \quad (8)$$

which, for our specific case, $A = 0.162289324$ and $B = -0.000665645$ for the best-fit parabola over all scans. To create a 3-D reference surface we use this best-fit 2-D parabola as a “parabola of revolution” about the z -axis which yields as our reference paraboloid for this dish:

$$z = A(x^2 + y^2) + B = 0.162289324(x^2 + y^2) - 0.000665645 \quad (9)$$

The benefit of having the mathematical expression, Eqn. 9, for the reference surface is that we may use it to calculate the z -coordinate value of the reference surface at any of our measured 3-D points to compare with the measured z -coordinate values at those points, the difference between the two giving the amount of deviation, in the z direction, of the reflecting surface at that point from the reference surface. We use Eqn. 9 as the reference surface in the next step to identify areas of the dish that may need mechanical adjustment to achieve better performance from the dish.

Step 3. Calculate deviations of the dish surface from the reference surface.

A useful method to view areas of the dish that deviate from a reference surface is to use a graphics program to create a 3-D color map from a list of points, each point being specified by 3 coordinates x , y , and z . Steps 1 and 2 provide a means to convert each of our measured points into such points for plotting. Rather than plotting the 3D points directly, which would simply create an image similar to that shown in Figure 2, it is more relevant to plot the points using the x , y coordinates of the measured points and the difference between z -values of the measured points and z -values of corresponding points on the reference surface.

Calculations and analyses of the deviations is straightforwardly accomplished by putting the measured data points and corresponding reference surface points into a spreadsheet from which common plotting programs can read the x , y , and z -deviations. In our case we use gnuplot¹¹ as the

plotting program to view the deviations of the dish surface from the reference surface. Figure 8 shows a 3-D image of the deviations of the dish surface from the reference surface including an x-y plane projection color map of the surface deviations.

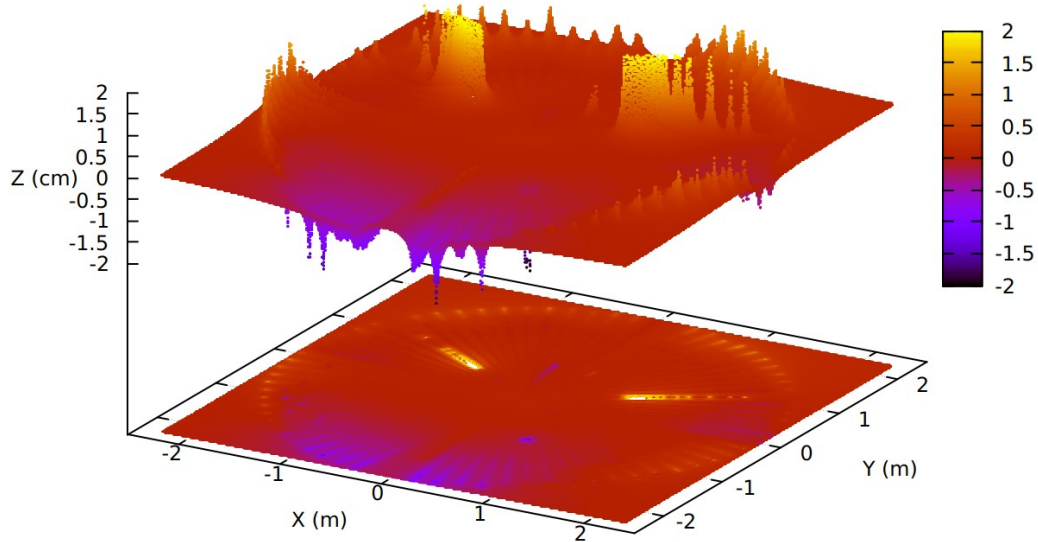


Fig. 8. A 3-D image showing deviations of the dish surface from the reference surface. A projection of the deviations is also shown on the x-y plane as a color map. The positions of the feed horn support beams is clearly evident in the image at 120-degree angle separations.

Figure 8 reveals that the uncorrected dish surface has significant-area deviations from the reference surface. Most deviations are shown to be in the 1-2 cm range above and below the reference surface. While this amount of deviation may seem small at first glance the fact that the deviations extend over a significant fraction of the reflecting surface is sufficient to seriously degrade the performance of the dish at 8.4 GHz.

Figure 9 superimposes the x-y color map projection of Fig. 8 onto a photograph of the dish to reveal where the deviation areas are located on the reflecting surface of the dish.

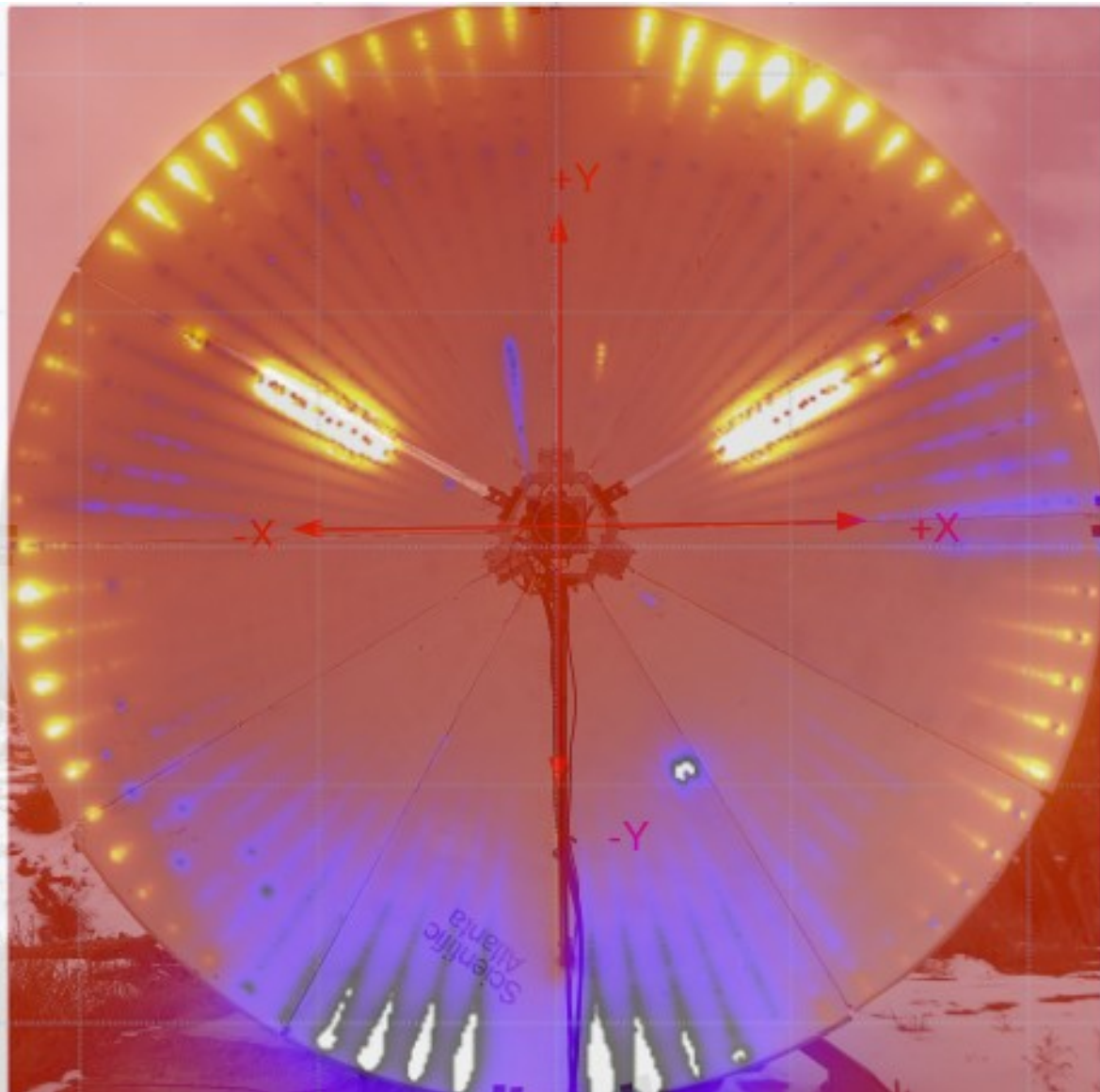


Fig. 9. Dish surface-deviations measured by the laser-rangefinder instrument are shown superimposed upon a photograph of the dish to reveal the areas of deviation, showing as blue/purple, that are significant deviations in terms of causing performance degradation of the dish. Areas showing as white surrounded by black within the blue/purple regions are off-scale regions of the plot in terms of magnitude toward the the blue direction (i.e., into the page in this view).

The areas of blue/purple need mechanical adjustment in a direction that is out of the page in this view to better match the reference surface and to thereby improve performance of the dish.

III. MODIFICATION OF CURVATURE OF THE DISH

Once the locations and magnitudes of the deviations of the dish surface from an ideal reference surface are known the task of mechanically correcting the deviations can be addressed. Methods

that can be used to correct surface deviations on a dish are many and varied but often involve adding one or more adjustable assemblies to the back side of the dish to apply stresses to the surface to force the local surface into a position that better matches a reference surface. Which adjustment method one might successfully apply to correct the surface curvature of a specific dish depends upon how the dish surface is constructed, how it is supported by its back structure, and what resources are available to be used to achieve the needed corrections. A review of possible methods that can be used for correction is beyond the scope of this document.

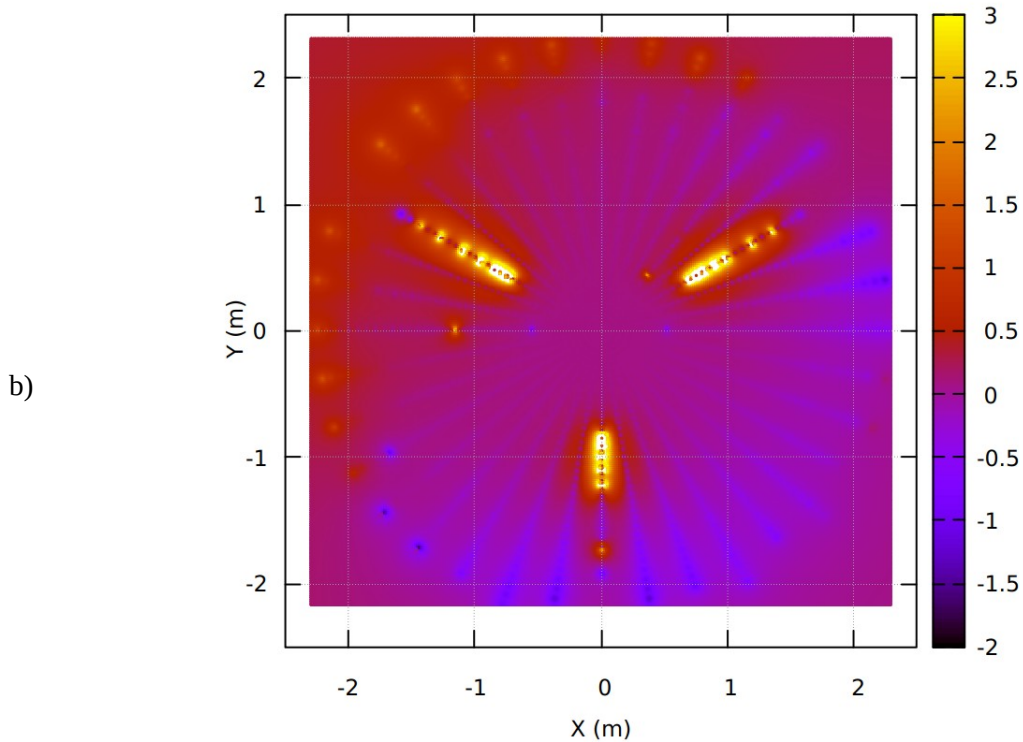
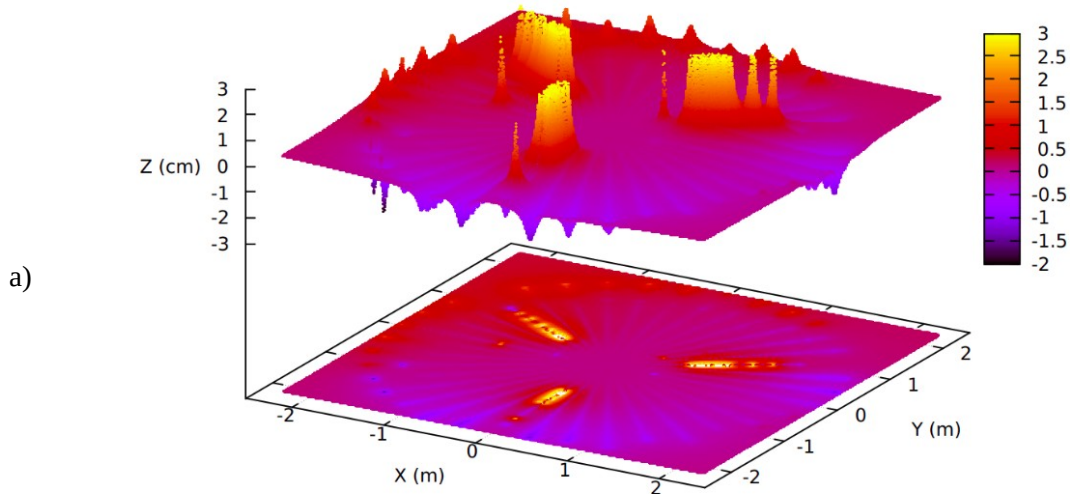
The dish we are working with has the characteristics that the surface is made from relatively thin aluminum and the steel back structure of the dish does not extend outward to the rim of the dish surface leaving the outer edges of the dish unsupported and susceptible to deformation if stresses are applied to the rim. This fact can be used in this case to introduce beneficial distortions in the curvature of the dish surface by applying stresses to the rim of the dish at selected positions on the rim to yield a better match the calculated reference surface.

As the most severe deviations in the surface of this dish are shown to be in a direction from front-side toward back-side the deviations in curvature can perhaps be corrected by applying torsion stresses at particular rim positions to pull the rim upward toward the feed horn position in those areas. Torsion stresses are introduced by attaching adjustable-length steel cables from the existing steel attachment points of the feed horn support beam bases on the front side of the dish to rim positions on the dish that correspond to the regions of largest deviation from the reference surface. The amount of stress introduced to the rim is adjustable by turnbuckles attached to the ends of the steel cables. We elected to use three torsion cables; two attached to the rim at the lower (bottom edge position in Fig. 9) edge position of the dish to the two steel upper feed horn support beam bases and one attached to the rim at the right edge of the dish to the left upper feed horn support beam base. The locations of the torsion cables are shown in Figure 10.



Fig.10. Image showing locations of the three torsion cables used to adjust curvature of the dish surface.

By adjusting tension on the torsion cables we are able to improve the match between the dish surface and the calculated reference surface. The improvement can be seen in the color map results from a new set of scans of the dish surface, shown in Figures 11a and 11b.



Figs. 11 a,b. Images showing that a more uniform match of the dish surface to the reference surface has been achieved by applying torsion stresses to the rim edges of this dish.

While adjustment of the surface curvature has not achieved a perfect match with the reference surface the total area containing deviations and the magnitudes of the deviations have been reduced, as seen by comparing Figs. 8,9 with Figs. 11a,b. Deviations across the dish are generally now no more than a centimeter different from the reference surface and less than a centimeter different over most of the dish surface. As we show in the next section adjusting the curvature of the dish achieved a significant improvement in performance of this dish at 8.4GHz.

IV. PERFORMANCE MEASUREMENTS

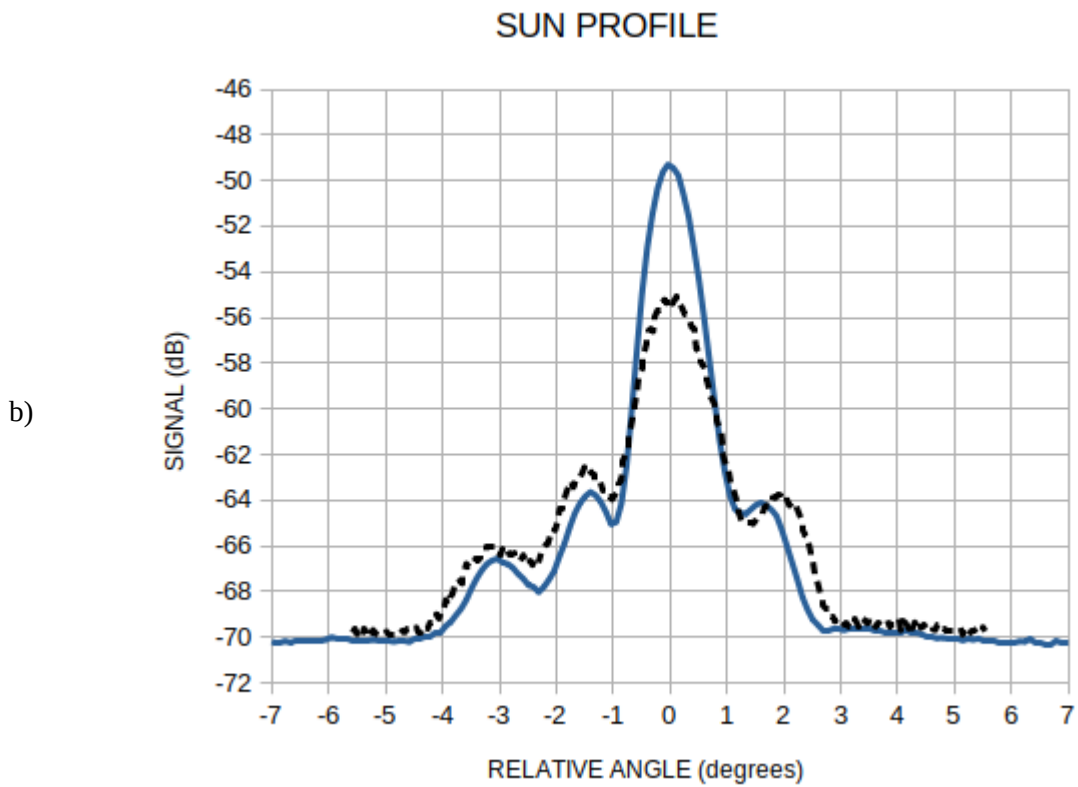
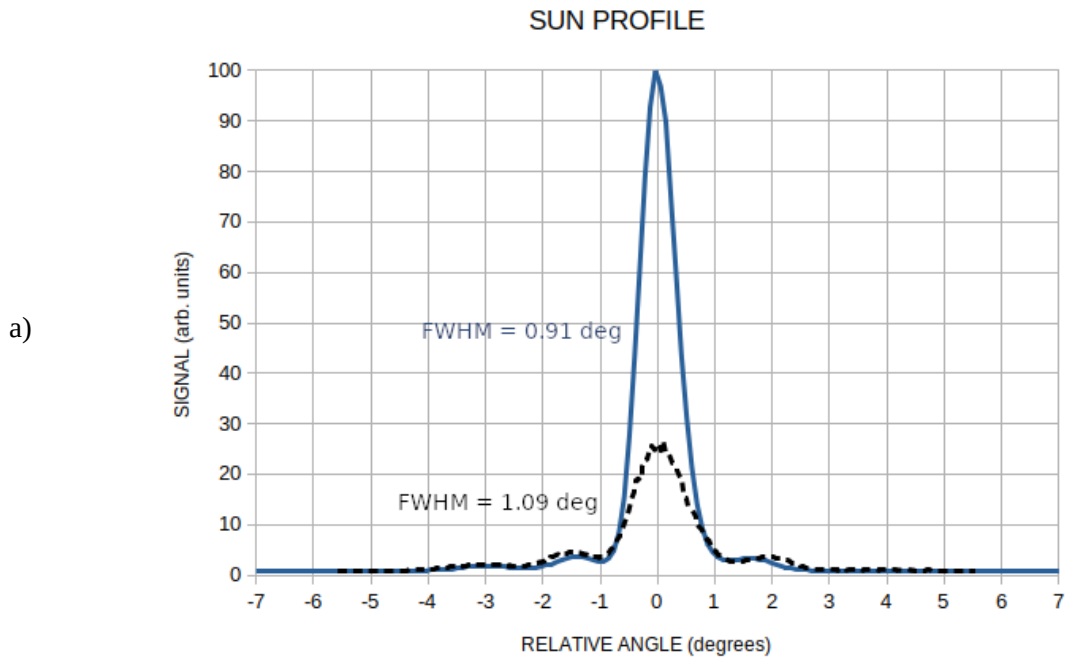
An important performance parameter for a parabolic dish antenna is the shape of the principal lobe of the antenna pattern of the dish, typically reported as the full-width-at-half-maximum (FWHM) of the angular profile of the principal lobe of the pattern, which we refer to here as Ω_{dish} . A convenient method of measuring dish pattern beam width is made by sweeping the pointing direction of the dish across the position of the sun in the sky to create an intensity profile as a function of pointing angle. If the sweep is performed by moving the azimuth angle of the dish the appropriate cosine correction due to the elevation angle must be applied to the measured profile, of course. No such correction is necessary for elevation angle sweeps.

In many cases, such a measured profile has an angular width approximately equal to the width of the principal lobe of the dish beam pattern. The method works well for dishes that have a principal lobe beam width much larger than the apparent angular width of the sun, Ω_{sun} , which at most frequencies used by amateur radio astronomers is about half a degree. When the width of the principal lobe of the dish pattern is nearly equal to or smaller than the angular width of the sun then it is important to recognize that the shape of the measured profile is an integral convolution of the beam pattern of the sun and the beam pattern of the dish, which results in a measured width that is always greater than either, and in many cases significantly greater than the width of the principal lobe of the dish pattern.

If it can be assumed that the primary lobe of the dish beam pattern and the emission pattern of the sun are both essentially Gaussian, which is usually a reasonable assumption, then a good estimate of dish beam width, Ω_{dish} , can be calculated from a profile scan of the sun by taking the square root of the difference of the squares of the angular width of the measured profile, Ω_{profile} , and the apparent angular width of the sun, Ω_{sun} , respectively. That is,

$$\Omega_{\text{dish}} = \text{sqrt}(\Omega_{\text{profile}}^2 - \Omega_{\text{sun}}^2) = \text{sqrt}(\Omega_{\text{profile}}^2 - (0.5)^2) = \text{sqrt}(\Omega_{\text{profile}}^2 - 0.25) \quad (10)$$

Figure 12a shows measured sun profiles, before and after the surface correction was applied, plotted on a linear scale to be able to easily determine the FWHM of the profiles. Figure 12b shows the same data plotted on a logarithmic scale to show the magnitude of the signal in terms of the power level of the profile peak relative to the base line noise floor. The difference between the magnitude of a peak and that of the noise floor is proportional to the gain of the dish in both plots, linear in the first and logarithmic in the second. However, it should be noted that the solar flux was somewhat higher on the day that the later profile was collected therefore the differences shown include contributions due to an increased solar flux on the later day measurement. A difference in the solar flux levels on the two days does not affect the validity of the beam width measurements but does influence the apparent gain values observed between the two days, giving a higher apparent gain value on the day with the higher solar flux.



Figs. 12a,b. Linear (12a) and logarithmic (12b) plots of profiles of the sun. The solid blue lines were collected on 20FEB2022 after the dish curvature was adjusted; the dashed lines show sun profiles collected on 12JUL2021 before curvature adjustment was made.

Using Eqn. 10 and Fig. 11a, the dish beam pattern FWHM before performing the adjustment of the surface curvature dish is:

$$\Omega_{\text{dish}} \text{ (before)} = \text{sqrt}(1.09^2 - 0.5^2) = \mathbf{0.97 \text{ degree}} \quad (11)$$

and after the curvature adjustment,

$$\Omega_{\text{dish}} \text{ (after)} = \text{sqrt}(0.91^2 - 0.5^2) = \mathbf{0.58 \text{ degree.}} \quad (12)$$

The above analysis of the plots in Figure 12 demonstrate that the dish beam-pattern width has been reduced by almost half as a result of adjusting surface curvature of this dish. The gain was also improved as a result of narrowing the beam pattern, of course, but not by as much as is suggested by the magnitudes of the respective before/after profiles due to the solar flux difference on the measurement days.

Figures 12a and 12b show the results of collecting profiles of the sun on two different widely separated days; 12JUL2021, before the surface curvature adjustment and 20FEB2022, after the surface curvature adjustment. The solar flux on those two days differed. In particular, the 10.7cm solar flux, in terms of spectral flux density, on 12JUL2021 and 20FEB2022 were 71.6 sfu and 97.1 sfu, respectively¹². Due to a combination of increased gain of the dish and higher solar flux on the later profile measurement day, the apparent gain of the dish appears to have increased by roughly a factor of 4 (i.e., about 6dB) as a result of adjusting the surface curvature. But such a quantitative conclusion is misleading and incorrect because solar flux was higher on the later measurement day relative to the earlier measurement day.

As mentioned, the 10.7 cm solar flux value on the later profile measurement day was about 30% higher than when the earlier profile was collected. Our experience at 1296 MHz with apparent gain varying due to variations of solar flux density in the 70-100 sfu range is that the apparent gain increases by about 1.5 dB for the amount of change in solar flux that existed between our profile measurements¹³, i.e. the apparent gain is expected to increase by roughly $10^{1.5} = 1.32$, or 32%, due to the increased level of solar flux on the later measurement day. Thus, assuming that the apparent gain versus solar flux behavior at 8.4 GHz is roughly similar to the behavior at 1296 MHz, our estimate of the additional gain of the dish resulting from the curvature change is about 6dB-1.5dB = 4.5 dB relative to the uncorrected dish, or conservatively, more than twice the gain of the uncorrected-surface.

We note that low-level asymmetry exists in the beam profiles but believe the level of asymmetry present is not significant with respect to the tasks this radio telescope is expected to perform.

V. SUMMARY

This document describes a 3-step procedure that can be used to measure the surface accuracy of parabolic dishes. Use of the procedure was demonstrated by applying it to a 4.63 meter diameter parabolic dish antenna, using a robotic-turret-mounted laser rangefinder assembled from commercially available components. A description was given of how the procedure is used to guide surface curvature modifications of the dish. It was shown that applying the procedure to guide modifications of the dish-surface curvature resulted in significant performance improvement of the dish at 8.4 GHz. While the amount of curvature correction applied to this dish may seem to be small in magnitude and perhaps not particularly important when using the dish at low frequencies it

was demonstrated that correction of surface curvature over the relatively large fraction of surface affected by the non-optimum curvature provides significant improvement for operations of this dish at 8 GHz.

VI. REFERENCES

1. Joe Martin is an amateur radio astronomer, retired from a scientific research career in Materials Science. He received the B.S. degree in Physics from U. of New Mexico (1979) and the M.S. and Ph.D. degrees in Materials Science from U. of Wisconsin (Madison) in 1979 and 1986, respectively. Dr. Martin served 12 years as a technical staff member and project leader at Los Alamos National Laboratory performing fundamental research in the areas of atomic scale surface science, energetic nanometer-scale materials, and high-temperature superconductivity. He has co-authored 30 refereed papers in various scientific journals and is a co-inventor on 7 U.S. patents. He is a co-founder of four nano-technology companies. Dr. Martin is an extra-class amateur radio operator, K5SO.

2. See, for example, David J. Rochblatt, "Microwave Antenna Holography", 1992, *IEEE Transactions on Microwave Theory and Techniques* 40(6):1294 – 1300.

Web access:

https://descanso.jpl.nasa.gov/monograph/series10/08_Reid_chapt8.pdf

3. See, for example, N. Udaya Shankar et al., "Photogrammetry Measurements of a 12-metre Preloaded Parabolic Dish Antenna", National workshop on the Design of Antenna & Radar Systems (DARS), February 13-14, 2009 ISRO Telemetry Tracking and Command Network (ISTRAC) Bangalore, India.

Web access: <https://arxiv.org/pdf/0905.1252.pdf>

4. See, for example, Edwin A. Bryce and Floyd H. Gallegos, "Compact-Range Coordinate System Established Using A Laser Tracker", Sandia Report SAND2006-7541, 2006, Sandia National Laboratories, Albuquerque, New Mexico 87185 and Livermore, California 94550.

Web access: https://digital.library.unt.edu/ark:/67531/metadc883768/m2/1/high_res_d/899721.pdf

5. See <https://www.fluke.com/en-us/product/building-infrastructure/laser-distance-meters/fluke-414d>.

6. See <http://www.porcupinelabs.com/lr4>.

7. See <https://www.robotshop.com/en/phantomx-xl430-robot-turret.html>.

8. Min Dai, Timothy S. Newman, Chunguang Cao, "Least-squares-based fitting of paraboloids" *Pattern Recognition* 40 (2007) 504-515.

9. E.L. Hall, J.B.K. Tio, C.A. McPherson, F.A. Sadjadi, "Measuring curved surfaces for robot vision", *IEEE Comput.* 15 (12) (1982) 42-54.

10. See the R computing language home page: <https://www.r-project.org/>

11. See the gnuplot home page: <http://www.gnuplot.info/>

12. See the DRAO 10.7cm daily flux archive:

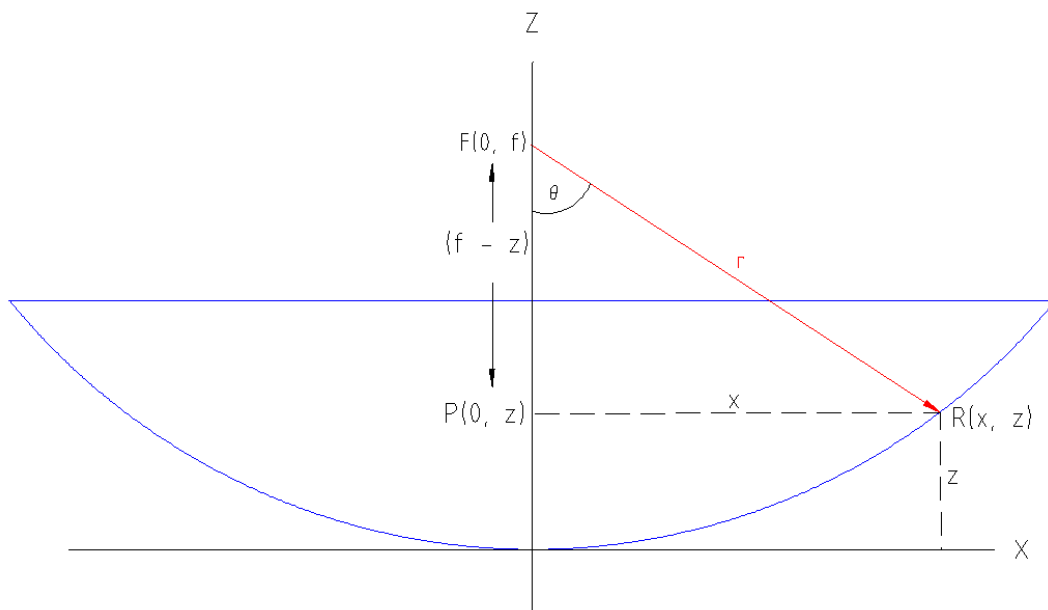
<https://www.spaceweather.gc.ca/forecast- prevision/solar-solaire/solarflux/sx-5-flux-en.php>

13. See <http://www.k5so.com/radio-astronomy/using-sun-noise.html> for our observed changes in measured sun noise at 1296 MHz with changes in 10.7 cm solar flux density.

14. See any analytic geometry text, as for example, “Calculus and analytic geometry”, Fourth Edition, by George B. Thomas, Jr., 1968, Addison-Wesley Publishing Company, Reading, Mass., page 333.

APPENDIX

A derivation of Eqn. (3) of the main text is facilitated by recognizing that all rim-to-rim scans across the surface of a perfect-surface parabolic dish trace a common parabola. The situation is depicted in the figure below. The blue lines represent a cross-section of the dish in the X-Z plane. Points F and R represent the focal point of the dish and a point on the dish surface, respectively. The red line of length, r , represents a laser rangefinder distance measurement path from point F to point R, and θ is the tilt angle of the turret during a scan.



The objective is to derive an expression for z in terms of r and θ only. From the figure it is seen that

$$z = f - r \cos(\theta). \quad (1)$$

Recall that the general formula for a parabola in the X-Z plane, in terms of its focal distance, f , is¹⁴

$$x^2 = 4f z. \quad (2)$$

Using the Pythagorean Theorem on the right-triangle FPR in the diagram,

$$r^2 = (f - z)^2 + x^2, \text{ or} \quad (3)$$

$$r = \text{sqrt}((f - z)^2 + x^2). \quad (4)$$

Substituting for x^2 from Eqn. (2),

$$r = \text{sqrt}((f - z)^2 + 4fz) = \text{sqrt}(f^2 - 2fz + z^2 + 4fz) = \text{sqrt}(f^2 + 2fz + z^2) = \text{sqrt}((f + z)^2)$$

yields

$$r = f + z. \quad (5)$$

Substituting for z from Eqn. (1),

$$r = f + f - r \cos(\theta) = 2f - r \cos(\theta) \quad (6)$$

and solving for f ,

$$f = (r + r \cos(\theta)) / 2. \quad (7)$$

Substituting for f in Eqn. (1),

$$z = ((r + r \cos(\theta)) / 2) - r \cos(\theta) = (r + r \cos(\theta) - 2r \cos(\theta)) / 2 = (r - r \cos(\theta)) / 2$$

and therefore

$$z = r (1 - \cos(\theta)) / 2 \quad (8)$$

Q.E.D.